Technical Notes

TECHNICAL NOTES are short manuscripts describing new developments or important results of a preliminary nature. These Notes cannot exceed 6 manuscript pages and 3 figures; a page of text may be substituted for a figure and vice versa. After informal review by the editors, they may be published within a few months of the date of receipt. Style requirements are the same as for regular contributions (see inside back cover).

Proportional Navigation vs an Optimally Evading, Constant-Speed Target in Two Dimensions

Paul M. Julich* and David A. Borg†
Louisiana State University, Baton Rouge, La.

Studies of differential games have indicated that for certain formulations proportional navigation constitutes the optimal pursuit strategy.[1] These formulations basically involve assumptions of a linear system with quadratic index of performance involving a weighting on the energy expended by pursuer and evader. This index has some justification during the initial study phase. Once a decision is made, however, to choose a particular guidance law for the pursuer (such as proportional navigation) the evader is no longer as concerned with the energy he consumes. A realistic index of performance is simply $J = -r^2(t_f)$, where $r(t_f)$ is the range at the time of closest approach t_f. In this Note we consider a two-dimensional, constant-velocity, point model of a target in an encounter with a pursuer in the horizontal plane (Fig. 1). Mechanization of proportional navigation introduces numerous effects not included in the differential game formulation. We will consider the effects of two constraints: 1) the lateral acceleration (in g's), $G_{P_{\max}}$; and 2) a time constant τ_p in the control system of the pursuer.

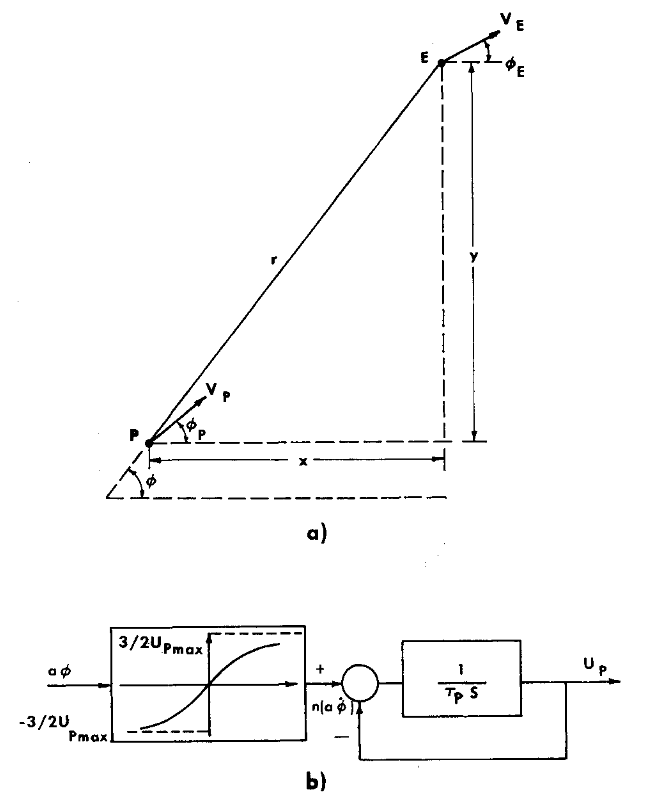

Fig. 1 Problem definition: a) problem geometry, b) pursuer's guidance system.

The chosen set of state variables x, y, ϕ_E and ϕ_P result in the following differential equations:

$$\dot{x} = V_E \cos\phi_E - V_P \cos\phi_P \tag{1}$$

$$\dot{y} = V_E \sin\phi_E - V_P \sin\phi_P \tag{2}$$

$$\dot{\phi}_P = U_P;\ \dot{\phi}_{E_{\max}} = U_{E_{\max}} U_E \tag{3}$$

where

$$|U_E| \leq 1 \text{ and } U_{E_{\max}} = gG_{E_{\max}}/V_E \tag{4}$$

These equations assume that the maximum number of g's, $G_{E_{\max}}$ the target may experience is limited. In ideal proportional navigation, $U_P \propto \dot{\phi}$, where ϕ is the line of sight from the pursuer to the target. However, with our two constraints, the simplified guidance system is assumed to be as shown in the block diagram, Fig. 1b. A nonlinear function limits U_P.

Although hard-limiting on G_P is desired, the application of hard limits causes discontinuities in derivatives needed for the optimization method used, so an approximation was made. The arc tangent function was chosen to approximate the hard limits. An additional differential equation illustrated in Fig. 1b governs the behavior of U_P:

$$\dot{U}_P = \frac{1}{\tau_P} U_{P_{\max}} \left(\frac{3}{\pi}\right) \tan^{-1}\left(\frac{3^{1/2} a\dot{\phi}}{U_{P_{\max}}}\right) - \frac{1}{\tau_P} U_P \tag{5}$$

where

$$\dot{\phi} = \dot{y}x - y\dot{x}/x^2 + y^2,\ U_{P_{\max}} = gG_{P_{\max}}/V_P \tag{6}$$

and a is the proportional navigation constant. At the ef-

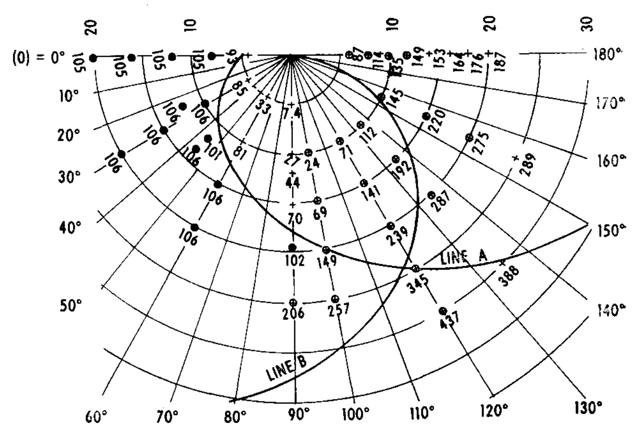

Fig. 2 Miss distance resulting from best control vs initial pursuer position; r(0) –K ft.

Received October 9, 1969; revision received June 22, 1970. This work was supported in part by the Armament Laboratory, Eglin Air Force Base, under contract F08635-68-C-0107, and in part by a Themis Grant, administered by the Air Force Office of Scientific Research, Contract F-44620-69-C-0021.

* Associate Professor, Department of Electrical Engineering.
† Graduate Student, Department of Electrical Engineering.

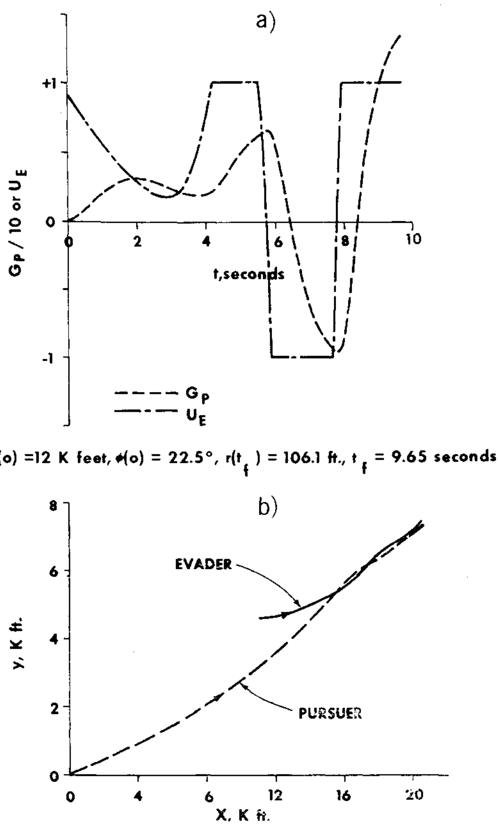

Fig. 3 Control and space trajectories for ϕ = 22.5°.

fective terminal time of the problem, when the pursuer has reached its closest approach to the evader, $\dot{r} = (\dot{x}x + y\dot{y})/(x^2 + y^2)^{1/2} = 0$.

The optimal control problem is: choose $U_E \epsilon U$, $U = \{U_E: |U_E| \leq 1\}$ so that $J = -r^2(t_f)$ is a minimum, subject to the differential side constraints, Eqs. (1–5).

There are five degrees of freedom $r(0)$, $\phi(0)$, $\phi_P(0)$, $\phi_E(0)$, and $U_P(0)$ in the specifications of the problem. By noting that it should always be possible to choose the axes used to write the system differential equations (see Fig. 1a) such that the x axis is parallel to $V_E(0)$ without effectively changing the results, $\phi_E(0)$ may be specified as zero without any loss of generality. It is assumed that the pursuer is aimed such that if neither the evader nor the pursuer applied any control, interception would occur. Thus, both evader and pursuer would follow straight line courses, and from the geometry of the problem, two of the initial conditions are specified in terms of other problem constants as follows:

$$U_P(0) = 0, \; \phi_P(0) = \phi(0) - \sin^{-1}[V_E/V_P \sin\phi(0)] \quad (7)$$

Using a steepest ascent procedure,[2] and calculating the control for various choices of $r(0)$ and $\phi(0)$ to obtain the maximum miss, points in Fig. 2 were calculated for the following case: V_E = 1013 ft/sec, V_P = 2252 ft/sec, $G_{E_{max}} = 5$, $G_{P_{max}} = 10$, τ_P = 0.5 sec, and a = 3.

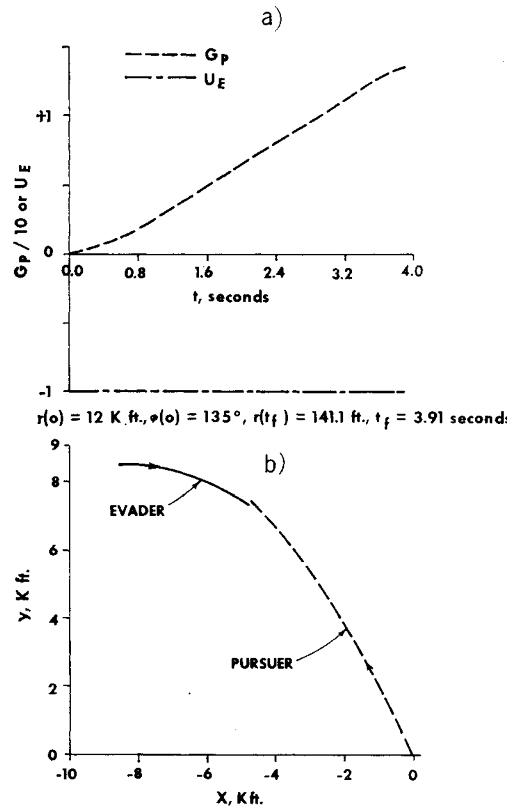

Fig. 4 Control and space trajectories for ϕ = 135°.

In Fig. 2, note that for each of the points marked with a solid circle $r(t_f) \simeq 106$ ft. For some of these points Table 1 gives $t_f - t_N$ the time increment between the last switching time t_N and t_f, as well as $t_N - t_{N-1}$ the time between t_N and the next to last switching time t_{N-1} of the best control for each of the initial conditions. Observe that $t_f - t_{N-1}$ for each case is ~4 sec. The best controls for the initial conditions in Table 1 are approximately the same shape as that for the initial conditions used to obtain Fig. 3.

Examination of numerous graphs of the nature of those in Fig. 3 for the initial conditions in Table 1 indicated that over the initial portion of the trajectory the evader maneuvers the pursuer such that the pursuer is behind him just preceding t_{N-1}. Using this observation, a computer program was written to calculate initial conditions where, if the evader applied +1 control until 4 sec before the problem terminated, the pursuer would be directly behind him at $t_f - 4$ sec. These initial conditions lie on line A in Fig. 2. Notice that the points in Table 1 lie outside of line A. For initial conditions close to or inside of line A in Fig. 2, the best control is bang-bang, and the resulting $r(t_f)$ is smaller than that of points outside line A.

Consider Fig. 4. For this initial condition the best control is $U_E(t) = -1$ for all $t \epsilon [0,t_f]$. The target turns toward the

Table 1 Initial conditions from Fig. 2 with approximately equal miss conditions

$\phi(0)$, deg	$r(0)$, Kft	$r(t_f)$, ft	t_f, sec	$t_f - t_N$, sec	$t_N - t_{N-1}$, sec
0	8	104.8	6.45	1.85	2.1
0	12	105.9	9.67	1.87	2.1
0	20	105.9	15.81	1.90	2.1
22.5	12	106.1	9.65	1.95	2.0
30	10	106.3	8.04	1.94	1.9
30	15	106.4	12.02	1.92	2.1
45	12	106.7	9.51	1.81	2.1
60	15	106.2	11.66	1.86	2.0
90	25	105.8	18.43 local max	1.83	2.0

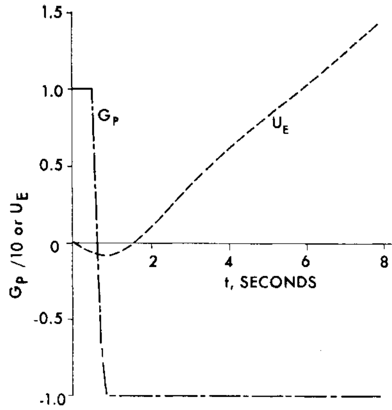

Fig. 5 Plot of costate variable $P\phi_E$ pursuer g's and evader control U for $r(0) = 25$ K ft, $\phi(0) = 155°$, $r(t_f) = 288.72$, $t_f = 7.93$ sec.

center of curvature of the pursuer's trajectory, because the effects of 1) the g limit on the pursuer 2) the fact that the proportional navigation system does not demand large responses from the missile over the initial portion of the trajectory, and 3) the time delay in the pursuer's guidance system, allow the target for some initial conditions to turn inside the pursuer's trajectory.

For initial conditions in Fig. 2 marked by a circled plus, the best control was $U_E(t) = -1$ for all $t\epsilon[0,t_f]$. Line B in Fig. 2 is a locus of initial conditions where, if the target applies -1 control for all $t\epsilon[0,t_f]$ he would collide with the pursuer if the pursuer had started on line B and had followed a straight line course of the point of interception. Notice that initial conditions marked by a circled plus lie in the vicinity of line B.

For the points marked by a plus which lie outside line B, the application of -1 control alone would not maneuver the evader to a point inside the pursuer's trajectory. Hence the evader applies $+1$ control to maneuver the pursuer to a point where the application of -1 control would result in termination inside the pursuer's path. The best control for these initial positions is bang-bang with only one switch and the control sequence is $(+1, -1)$, for example, see Fig. 5.

Figure 2 presents only the maximum miss obtained for each of the initial conditions. It is interesting to note that for some points local maximums were obtained for each of the above control philosophies.

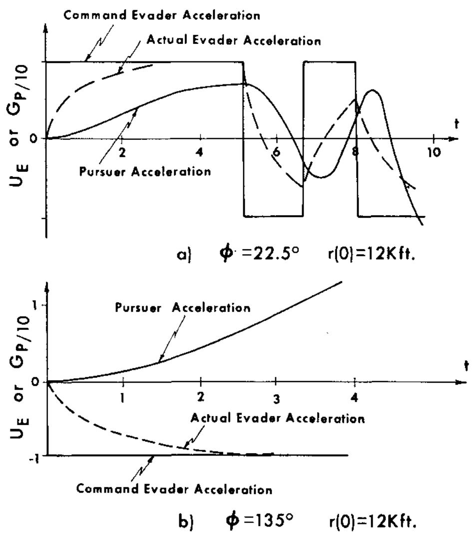

Fig. 6 Accelerations of pursuer and evader if evader time constant of 1 sec is assumed.

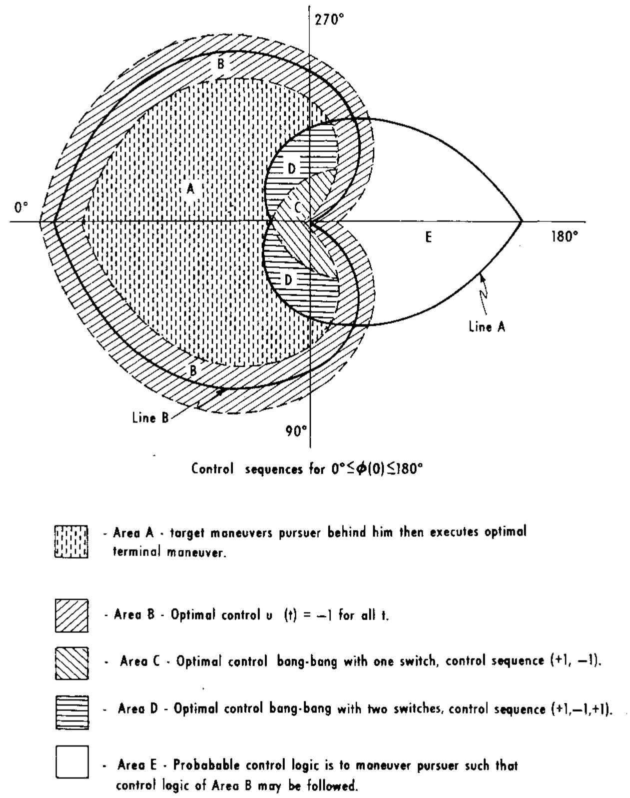

Fig. 7 Target control sequence for given pursuer initial positions.

Comments

An interesting observation from the included results is the change of evasive strategy with $r(0)$ and $\phi(0)$. This is not apparent from the solution of the differential game formulation.[3] The oscillatory behavior exhibited by the target is, of course, due to τ_P. As a practical fact, the mathematical model of a differential game is seldom realized exactly. Problems of this nature thus warrant additional study as differential game theory becomes more popular.

It is noteworthy that certain assumptions necessary for linearization of the evasive problem,[4] e.g., the assumptions that 1) angular deviations from $\phi(0)$ are small and 2) t_f is approximately independent of evasive maneuvers, are not satisfied for most cases. In fact, the basic strategy of the target is to maneuver initially so as to structure the encounter in his favor. In other words, the initial maneuver is intended either to decrease t_f by turning toward the pursuer or to increase t_f by turning away. Thus for large r, the problem always degenerates into a tail chase or a head-on encounter.

The model outlined in this paper assumes that the evader has direct control of his lateral acceleration, and thus the model is not directly applicable to an aircraft (evader)-missile (pursuer) engagement. The inclusion of a time constant τ_E in the evader's control system would be a first step in modeling this type of encounter. The authors have extensively studied this case also. The results are different quantitatively from those presented herein, but a good correlation can be shown between the results of the two cases (compare Fig. 3a with 6a and Fig. 4a with 6b). The evasive principles outlined herein remain unchanged despite the introduction of a $\tau_E(\tau_E = 1)$. The evader still performs an initial maneuver to structure the encounter in either the head-on or tail-chase mode and follows this with a weave or break maneuver. He still uses maximum commanded g turns, although his actual lateral acceleration seldom reaches $G_{E_{\max}}$. The introduction of τ_E, however, adds another variable that obscures the basic trends which appear. Thus the basic results are presented with $\tau_E = 0$.

Sensitivity studies have also been conducted for the parameters involved in the problem.[5] These different choices of pursuer's constants show that the optimum values of $t_f - t_N$ for initial conditions in area A of Fig. 7 vary with the choice of missile parameters, and that the shape and size of all the areas of control philosophies are affected by these choices. Generally an increase in a or $G_{P_{max}}$ or a decrease in τ_P reduces $r(t_f)$. The velocities, however, enter the picture in a much more interesting manner. It appears in fact that for a given V_E there is an optimum V_P. This will be reported on at a later date.

In closing, it should be noted that the research conducted considered only $0 \leq \phi(0) \leq 180°$. However, the problem is symmetrical, and for $180° \leq \phi \leq 360°$ it is only necessary to use the negative of the control sequence. Figure 7 summarizes the results of the investigation. It is not claimed that the areas in this graph represent the actual size or shape of the true areas of target control philosophies. The initial conditions actually investigated for this graph include only the vicinity of the area enclosed by the intersection of line A and B, as may be seen by examining Fig. 2. The extensions are reasonable guesses.

References

[1] Ho, Y. C., Bryson, A. E., Jr., and Baron, S., "Differential Games and Optimal Pursuit-Evasion Strategies," *IEEE Transactions on Automatic Control*, Vol. AC-10, No. 4, Oct., 1965, pp. 385–389.

[2] Balakrishnan, A. V. and Neustadt, L. N., *Computing Methods in Optimization Problems*, Academic Press, New York, 1964, pp. 71–77.

[3] Bryson, A. E., Jr. and Ho, Y. C., *Applied Optimal Control*, Blaisdell, Waltham, Mass., 1969, pp. 287–288.

[4] Harvey, C. A., "Optimal Evasion (in Case Proportional Navigation is the Pursuit Strategy)," Appendix C, "The Calculus of Aerial Combat," R-RD 6418, May 1969, Honeywell Systems and Research Division, Minneapolis, Minn.

[5] Julich, P. M. and Borg, D. A., "Effects of Parameter Variations on the Capability of a Proportional Navigation Missile Against An Optimally Evading Target in the Horizontal Plane," LSU-T-TR-24 (thesis), 1969, Louisiana State Univ., Baton Rouge, La.

Pulse Heating and Equilibration of an Insulated Substructure

P. J. Schneider* and C. F. Wilson Jr.†
Lockheed Missiles and Space Company
Sunnyvale, Calif.

Nomenclature

c = specific heat, Btu/lb-°F
D = pulse heating duration, sec
Fo_i' = modified Fourier number = $\alpha_i D/2\pi\delta_i^2$, $i = 1,2$
k = thermal conductivity, Btu/sec-ft-°F
n,n' = $\rho_2 c_2 \delta_2/\rho_1 c_1 \delta_1$ and $\rho_2 c_2 k_2/\rho_1 c_1 k_1$, respectively
Q'' = total heat input = $q''_{max} D/2$, Btu/ft²
q'' = instantaneous heat input, Btu/sec-ft²
T = dimensionless temperature rise = $(k_1/\delta q''_{max} Fo_1')(t - t_0)$
t = plate temperature, °F
t_{eq} = equilibrium temperature = $t_0 + \pi\delta_1 q''_{max} Fo_1'/(n+1)k_1$, °F
X = x/δ_1; x = depth from heated face, ft
α = thermal diffusivity = $k/\rho c$, ft²/sec
δ = thickness, ft
Θ = $2\pi(\theta/D)$; θ = time, sec
ρ = density, lb/ft³

Subscripts

eq = equilibrium
max = maximum
0 = initial value ($\theta \leq 0$)
1,2 = outer and inner layers, respectively

Introduction

A HEAT-CONDUCTION problem that recurs in aerospace systems design involves exposure of a two-layer plate to symmetrical pulse heating of the form

$$q'' = q''_{max} \sin^2 \pi\theta/D \quad (1)$$

Usually the outer layer is of lower thermal conductivity than the inner load-bearing layer. As such, significant temperature gradients develop only in the outer insulation and the inner substructure can be taken to respond isothermally (Fig. 1). Examples include ascent-phase aerodynamic heating of rocket boosters and payloads, aerodynamic heating of re-entry vehicles, and flash heating of objects such as near exposure to nuclear detonations. These applications encompass such large excursions in environment, material properties, and individual layer thicknesses that it was deemed worthwhile to solve the two-parameter problem, including post-heating equilibration, in a general manner.

Analytical Model

The dimensionless differential equations and boundary conditions for the constant-property, two-layer plate system with no surface decomposition or surface reradiation, a high-conductivity inner layer ($k_2 \rightarrow \infty$), and an adiabatic rear face are:

$$\Theta \leq 0 \text{ (initial condition)};\ T_1 = T_2 = 0, \quad 0 \leq X \leq 1 \quad (2)$$

$0 < \Theta \leq 2\pi$ (pulse heating);

$$\partial T_1/\partial X = -(1/Fo_1')\sin^2\Theta/2, \quad X = 0 \quad (3)$$

$$\partial^2 T_1/\partial X^2 = (1/Fo_1')\partial T_1/\partial\Theta, \quad 0 < X < 1 \quad (4)$$

$$T_1 = T_2, \quad X = 1 \quad (5)$$

$$\partial T_1/\partial X = -(n/Fo_1')\partial T_2/\partial\Theta, \quad X = 1 \quad (6)$$

$2\pi < \Theta \leq \Theta_{eq}$ (adiabatic equilibration); Eqs. (4–6) apply, and

$$\partial T_1/\partial X = 0, \quad X = 0 \quad (7)$$

The three dimensionless variables are T, X, and Θ, and the two dimensionless parameters are Fo_1' and n. The more general case of finite k_2 introduces a third free parameter n'. Equations (2–7) refer to the special case of large k_2 where $n' \rightarrow \infty$. Low values of n correspond to thick insulation δ_1 or insulation with large ρc relative to the underlying substruc-

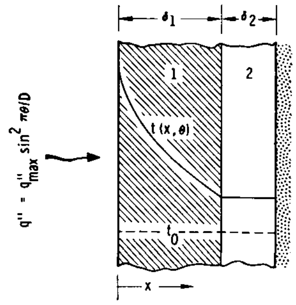

Fig. 1 Two-layer plate.

Presented as Paper 70-14 at the AIAA 8th Aerospace Sciences Meeting, New York, January 19–21, 1970; submitted February 11, 1970; revision received June 25, 1970.

* Staff Engineer, Missile Systems Division.
† Senior Thermodynamics Engineer, Aero-Thermodynamics, Missile Systems Division.